Values of L_{20} and L_{seq} for tunnels in Norway

Kai Sørensen, 13 August 2018

Foreword

This report is prepared in accordance with an agreement in the NMF group for road and tunnel lighting.

Introduction

Values of L_{20} and L_{seq} of tunnels in Norway have been measured by Pål Johannes Larsen, Norconsult by means of a calibrated luminance camera. These, and a number of other data, are introduced in section 1, while table A.1 in annex A provides the actual values. The pictures obtained with the camera are shown in annex B.

Both of the values L_{20} and L_{seq} apply for an observer at a distance in front of a tunnel portal and an observation direction towards the centre of the tunnel opening and both of the values represent the glare caused by the surrounding to the tunnel portal.

L_{20} is the average luminance of the surroundings within a cone with a cone angle of ±10° about the observation direction.

L_{seq} is the veiling luminance caused by a wider field of the surroundings and determined as $5{,}1\times10^{-4}$ times the sum of the luminance values in the polar diagram of figure 6.2.2 in CIE 88:2004.

It is noted that contributions to the L_{seq} value from scattering in the atmosphere and in the windscreen can be added to form a total L_{seq} value. Additionally, the transmission through the windscreen can be taken into account. However, such modifications are not considered in this report.

L_{20} values are traditionally used to determine the luminance L_{th} of the threshold zone in the tunnel by means of k factors as provided in table 5.4 in CIE 88: 1990. For this purpose, the L_{20} values are determined for an observer position at the stopping distance from the tunnel portal.

At a stopping distance of 60 m, the k factor has a value of 0,05 for a symmetrical lighting system and a value of 0,04 for an asymmetrical lighting system – which is assumed to provide a better contrast of objects to the road surface. For longer stopping distances, the k factors are up to twice as high.

L_{seq} values are used to provide alternative values of the L_{th} in a fairly complex manner. However, L_{seq} values can be considered to be alternatives to L_{20} values, that take variations of the luminance of the surroundings better into account than L_{20} values.

In this simplified point of view, it is interesting to note that L_{seq} equals $0{,}055\times L_{20}$, when the surroundings have a uniform luminance. The factor may be somewhat higher or lower in real cases depending on actual variations of the luminance of the surroundings.

Accordingly, the L_{th} values for a stopping distance of 60 m need to be approximately equal to the L_{seq} values. This demonstrates that the lighting of the threshold zone serves to counteract disability glare by raising the L_{th} value to approximately the L_{seq} value.

For longer stopping distances, the L_{th} value needs to be up twice the L_{seq} value. The reason is the simple that an object is less visible at a longer distance.

In any case, it is interesting to compare L_{20} and L_{seq} values for actual tunnels in order to judge the benefit of using L_{seq} as compared to L_{20}. This is done in section 2 for both the actual stopping distances and for shorter distances of 3/4 , 2/4, and 1/4 of the actual stopping distances.

The values of L_{seq} and L_{20} at the stopping distance correlate with a regression line is given by $L_{seq} = 0{,}054 \times L_{20}$. This factor is close to the above-mentioned factor of 0,055 for the case of uniform luminance of the surroundings.

However, there are deviations from this regression line for the individual tunnel portals. The standard deviation is by a factor of 1,15, while twice the standard deviation is given by a factor of $1{,}15^2 = 1{,}33$. Accordingly, deviations can be expected to be within 33 % and -25 % in most cases.

If assuming that the L_{seq} value reflects the drivers need for lighting level in the threshold zone, then a setting based on the L_{20} value may result in errors of the lighting level at the tunnel portal of the above-mentioned percentages (33 % too high or 25 % too low).

For shorter distances, the deviations are larger.

It is interesting to study the decrease of the L_{seq} value with the distance during the approach to the tunnel portal, as this may relate to a gradual decrease of the lighting level in the threshold zone. This is done in section 3, where an average relative curve is derived.

1. Introduction to the values

Table A.1 in annex A provides values of L_{20} and L_{seq} and other data for 26 tunnel portals in Norway. For each tunnel portal the following is provided:

- the name of the tunnel and the orientation of the portal,
- the stopping distance,
- the percentage of sky included in the calculation of L_{20},
- the percentage of sky included in the calculation of L_{seq},
- the direction of driving towards the tunnel portal,
- values of L_{20} at the stopping distance in front of the tunnel portal,
- values of L_{20} at distances of 3/4, 2/4 and 1/4 of the stopping distance
- values of L_{seq} at the stopping distance in front of the tunnel portal,
- values of L_{seq} at distances of 3/4, 2/4 and 1/4 of the stopping distance.

In 11 cases, the data include both of the portals of a tunnel, while in 4 cases only one of the portals of a tunnel is included.

The stopping distance is either 60, 80 or 100 m. In Norway, this corresponds to driving speeds of respectively 60, 70 and 80 km/h.

Values of L_{20} and L_{seq} at the stopping distance have been determined on the basis of pictures taken with a calibrated luminance camera taken from that distance. Refer to figure 1, which shows the rings of the polar diagram of figure 6.2.2 in CIE 88:2004. The pictures are shown in annex B.

Values of L_{20} and L_{seq} at the shorter distances have been obtained from the same pictures by expanding the pictures in proportion to the rings.

The percentages of sky have been determined from the pictures as well.

The data does of course reflect given points in time.

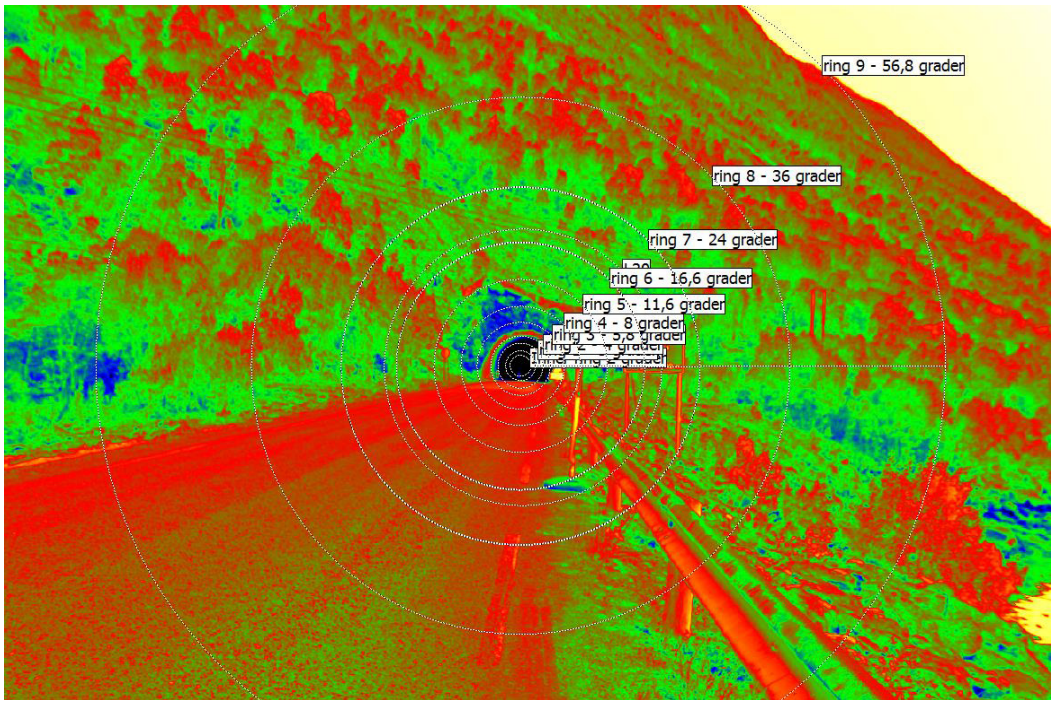

Figure 1: A digital photo with rings used for the calculation of L_{20} and L_{seq} values.

2. Comparison of L_{20} and L_{seq} values

The values of L_{20} and L_{seq} at the stopping distance correlate as shown in figure 2, where a regression line given by $L_{seq} = 0{,}054 \times L_{20}$ is also shown.

The standard deviation from the regression line is by a factor of 1,15. The majority of cases stay within twice the standard deviation given by a factor of $1{,}15^2 = 1{,}33$, so that deviations are between 33 % and -25 %. Lines corresponding to these deviations are also shown in figure 2.

If assuming that the L_{seq} value reflects the drivers need for lighting level in the threshold zone, then a setting based on the L_{20} value may result in errors of the lighting level at the tunnel portal of the above-mentioned percentages (33 % too high or 25 % too low).

The values of L_{20} and L_{seq} at all of the distances in front of the tunnel portal are compared in figure 3, which includes the above-mentioned lines. It is seen that the correlation between of L_{20} and L_{seq} remains good, when including all the distances, but with a somewhat larger spread.

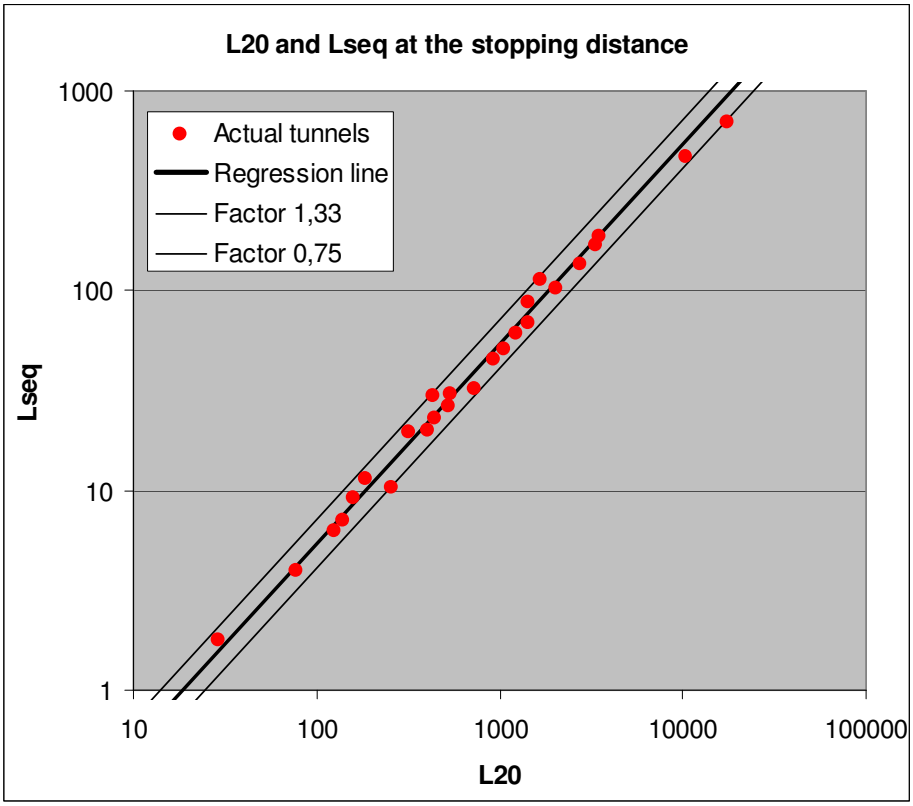

Figure 2: Comparison of values of L_{20} and L_{seq} at the stopping distance.

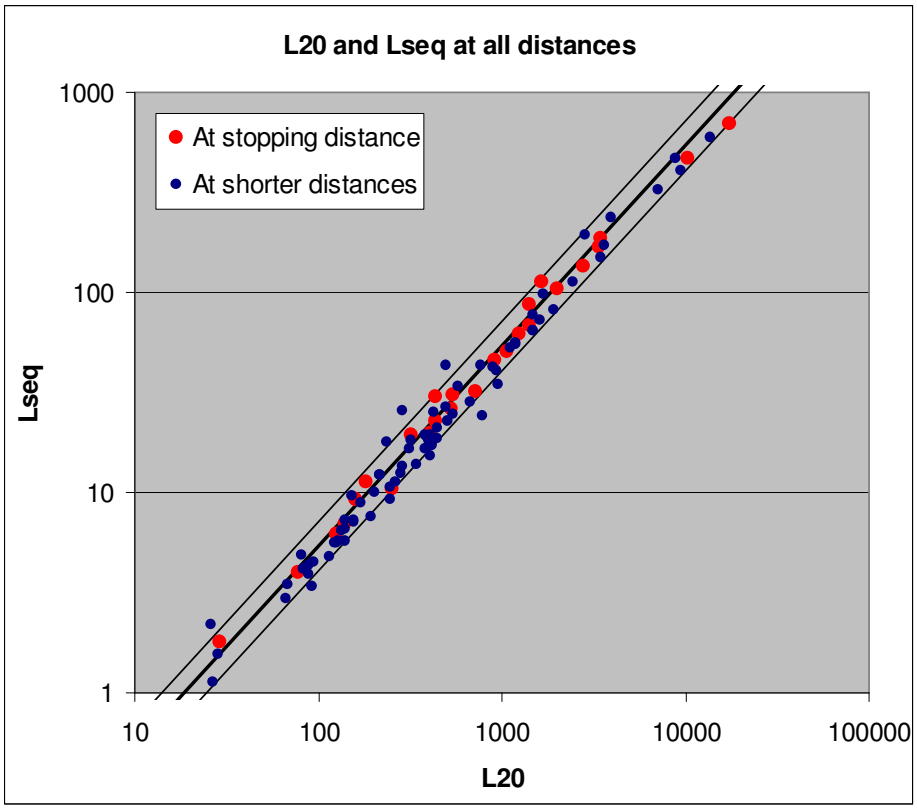

Figure 3: Comparison of values of L_{20} and L_{seq} at all the distances.

3. Variation of the L_{seq} values during the approach to the tunnel portals

Figure 4 shows the variation of the L_{seq} value with the distance for all of the tunnel portals.

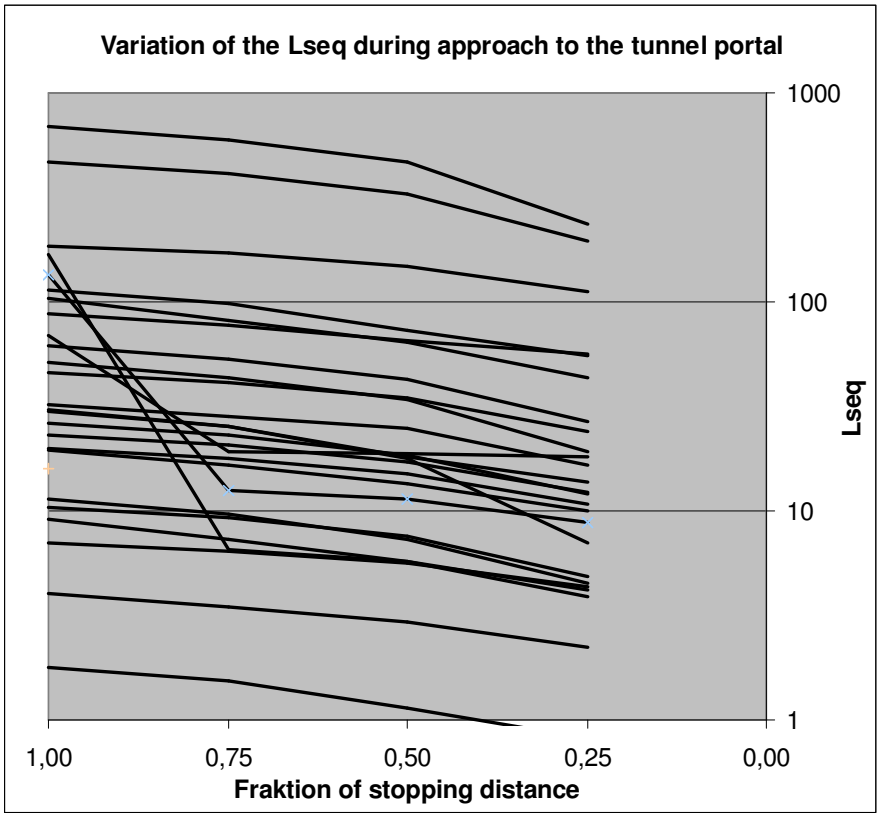

Figure 4: Variation of the L_{seq} with distance.

It is seen that the L_{seq} value is at its maximum at the stopping distance, and that it decreases during the first three quarters of the drivers approach towards the tunnel portal. The driver will experience a further decrease during the last quarter of his approach - in principle to naught - when considering only glare caused by the surroundings to the tunnel portal. Some glare from the lighting installation in the entrance zone will appear gradually, but at a relatively low level.

This offers the option to reduce the lighting level in the threshold zone gradually, starting already just behind the entrance portal and decreasing to a low level at the end of the threshold zone.

However, there is a limit to how much the lighting level should be reduced during the few seconds it takes for the driver to reach the tunnel portal. The standard reduction in accordance with CIE 88: 1990 is to 60 % - independent of the stopping distance. Another point of view may lead to much stronger reductions, corresponding to for instance a factor of 10 during a drive of 5 seconds.

If taking the other point of view, one can be interested in the relative decrease of the L_{seq} value, and this is shown in figure 5 for all the tunnel portals.

In a few cases, there is a strong initial decrease. These are labelled “extreme cases” in figure 5 and are shown in red. These cases are those of Brekk Vest, Brekk East and Mansfjell East. The pictures in annex B (respectively B.5, B.6 and B.9) seem not to provide any clue to why these cases are different from other cases.

Most cases show a gradual relative decrease down to values between 23 % and 65 %. The average is approximately 50 %. These cases are labelled “normal cases” in figure 5.

Figure 6 shows only the “normal cases” but gives in addition the average curve for those. The actual values for this curve are 1,0; 0,87; 0,70 and 0,48 for respectively the full stopping distance and the above-mentioned fractions of this stopping distance. It may be that this curve can serve as a standard curve when designing the lighting of the threshold zone.

.

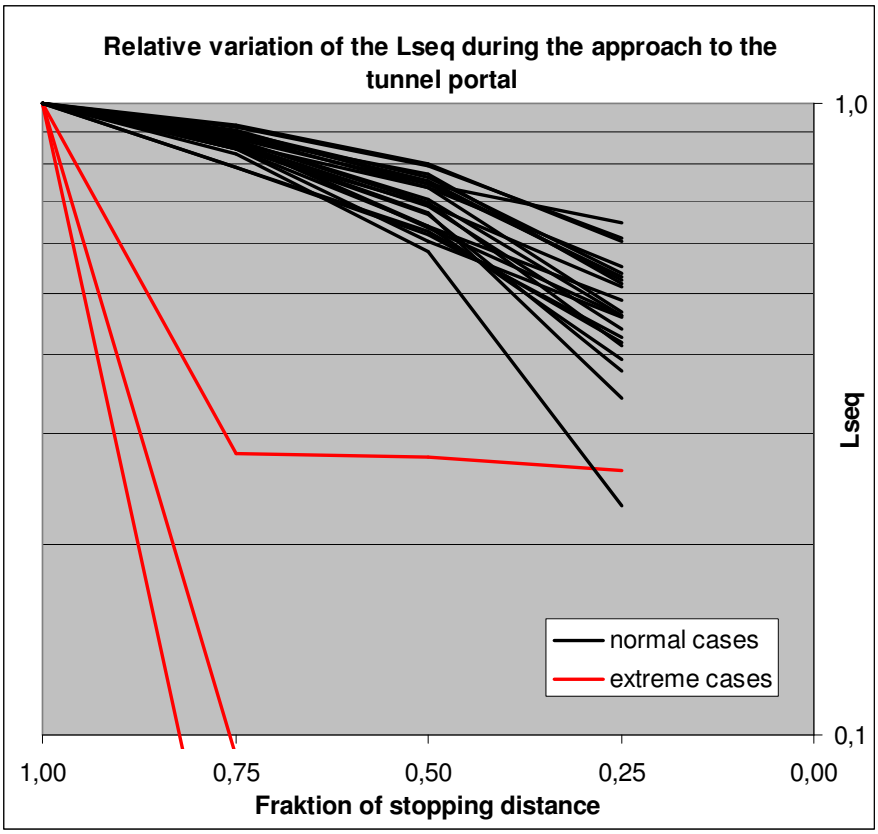

Figure 5: Relative variation of the L_{seq} with distance with an indication of extreme cases.

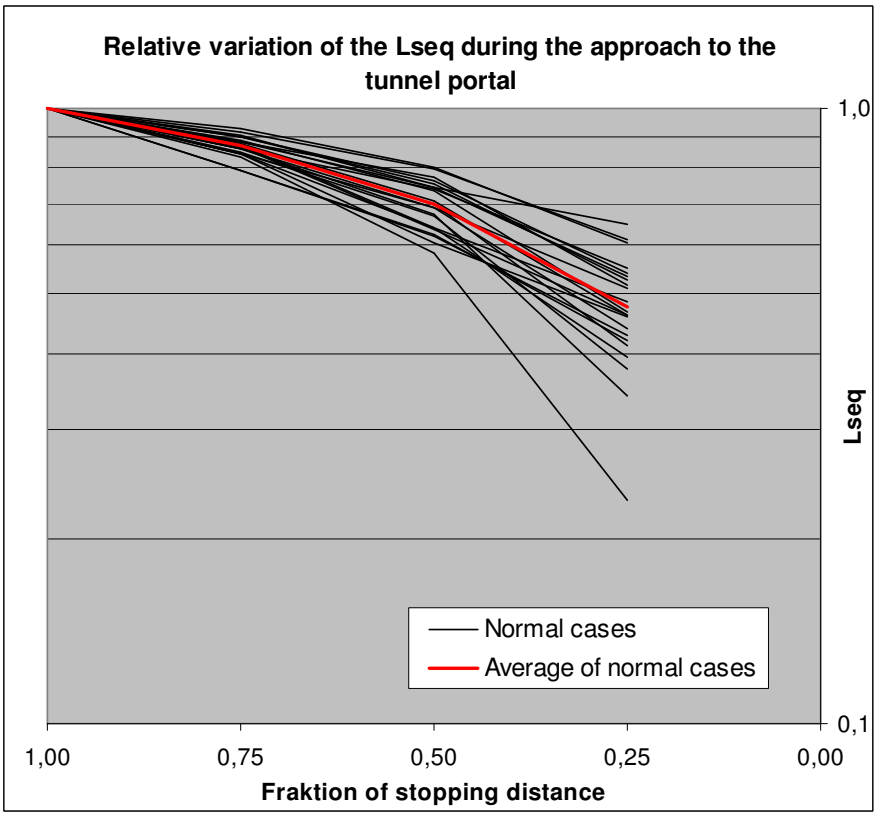

Figure 6: Relative variation of the L_{seq} with distance with the average of normal cases..

Annex A: Data for tunnels

Table A.1: Data for tunnels.

	Bømlafjord		Hordvik		Brekk		Buvik	Mansfjell		Løren	Storehaug		Saksenvik	
Tunnel	N	S	V	E	E	V	V	E	V	E	S	N	S	N
Stopping distance [m]	100	100	80	80	100	100	100	100	100	60	100	100	100	100
L_{seq} sky component	0%	0%	10%	5%	0%	10%	30%	5%	0%	30%	30%	30%	5%	20%
L_{20} sky component	0%	0%	0%	0%	0%	0%	5%	0%	0%	10%	5%	0%	0%	0%
Driving direction [0-360] degrees	135	355	100	225	225	45	55	290	135	0	350	190	190	315
L_{20} at stopping distance	1658	3464	2025	726	1427	3375	1061	441	2764	1233	10340	17380	925	1420
L_{20} at 3/4 stopping distance	1683	3620	1904	676	382	139	762	447	281	1120	9567	13850	929	1467
L_{20} at 2/4 stopping distance	1611	3480	1483	538	392	129	575	415	265	893	7120	8862	956	1473
L_{20} at 1/4 stopping distance	1193	2425	495	382	320	83,8	409	217	171	503	2825	3923	779	1186
L_{seq} at stopping distance	113,7	185,9	103,2	32,0	68,9	169,6	51,1	22,9	135	61,3	469	693	45,6	87,1
L_{seq} at 3/4 stopping distance	98,8	172,1	81,6	28,2	19,2	6,5	43,5	20,8	12,5	52,9	410	594	40,9	76,6
L_{seq} at 2/4 stopping distance	72,6	148,8	64,5	24,7	18,9	5,7	34,0	17,1	11,3	42,2	327	465	34,4	64,8
L_{seq} at 1/4 stopping distance	55,3	112,3	43,3	16,6	18,1	4,2	19,3	12,2	8,8	26,9	193	237	24,0	56,3

Brokløysa		Damsgård	Fannefjord		Ibestad	Ryggedal		Nesset		Finneidfjord	
V	E	V	V	E	N	V	E	S	N	S	N
80	80	60	100	100	80	100	100	100	100	100	100
20%	0%	0%	30%	15%	15%	5%	5%	15%	15%	15%	30%
5%	0%	0%	10%	0%	5%	0%	0%	0%	0%	0%	10%
90	225	225	60	230	300	135	290	170	350	160	10
183	125	254	77,7	29,0	525,6	140	408	321	436	159	539
152	122	245	68,1	28,4	507	134	413	313	425	157	290
141	114	194	66,8	26,9	449,3	125	406	290	402	142	239
95,5	93,2	81,0	26,1	15,0	215,4	88,4	250	203	344	87,8	156
11,3	6,2	10,4	4,0	1,8	26,2	7,0	19,8	19,5	30,0	9,2	30,5
9,6	5,6	9,2	3,4	1,5	22,9	6,4	17,9	16,5	25,3	7,3	25,4
7,3	4,7	7,6	3,0	1,1	18,5	5,6	15,2	13,5	18,2	5,7	17,8
4,5	3,4	4,8	2,2	0,8	12,1	4,3	10,7	10,0	13,7	3,9	7,1

Annex B: Pictures obtained with the camera

Figure B.1: Bømlafjord North

Figure B.2: Bømlafjord South

Figure B.3: Hordvig West

Figure B.4: Hordvig East

Figure B.5: Brekk West

Figure B.6: Brekk East

Figure B.7: Buvik East

Figure B.8: Mansfjell East

Figure B.9: Mansfjell West

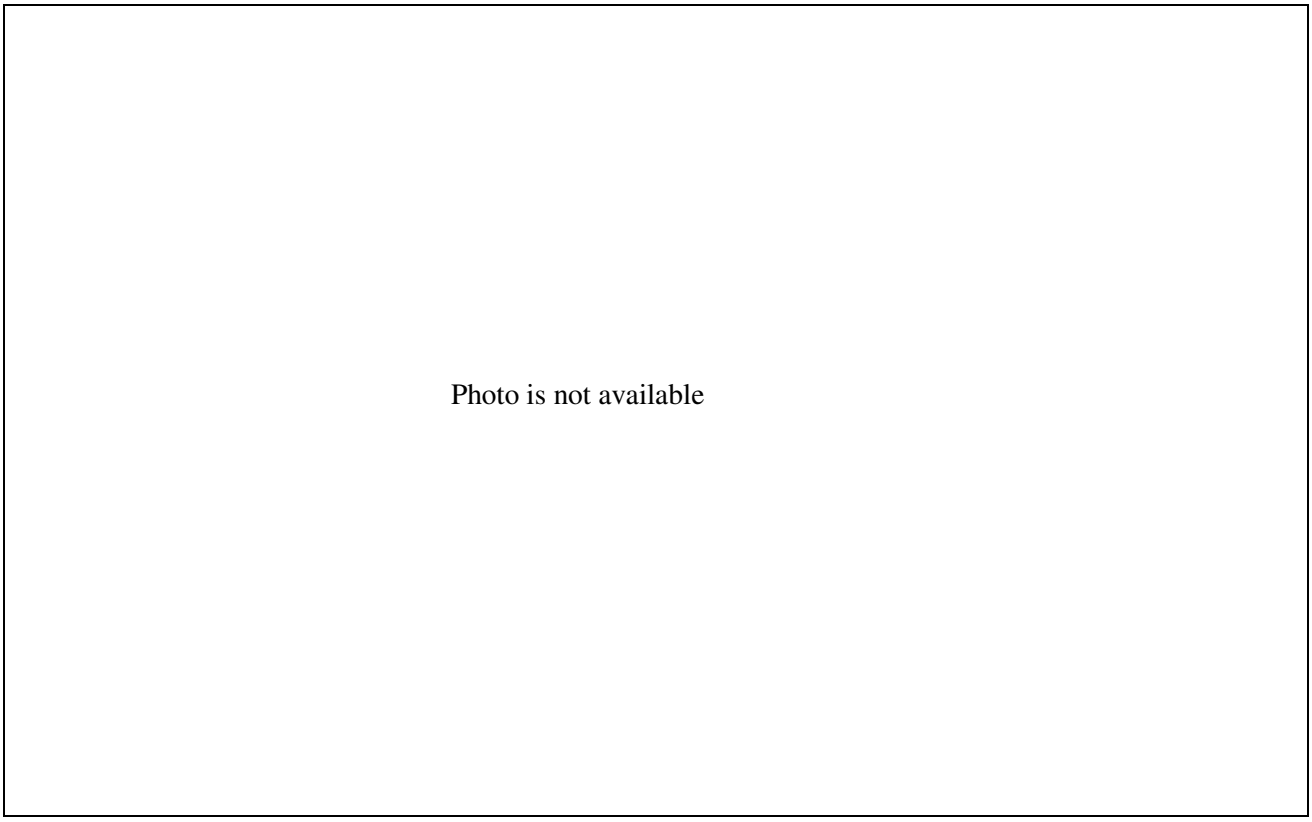

Figure B.10: Løren East

Figure B.11: Brokløysa West

Figure B.12: Brokløysa East

Figure B.13: Damsgård West

Photo is not available

Figure B.14: Fannefjord West

Figure B.15: Fannefjord East

Figure B.16: Ibestad N

Figure B.17: Ryggedal East

Figure B.18: Storehaug South

Figure B.19: Storehaug North

Figure B.20: Saksenvig South

Figure B.21: Saksenvig North

Figure B.23: Nesset South

Figure B.24: Nesset North

Figure B.25: Finneidfjord South

Figure B.26: Finneidfjord North